第 30 卷第 1 期 无 机 化 学 学 报 Vol.30 No.1
2014 年 1 月 CHINESE JOURNAL OF INORGANIC CHEMISTRY 204-212

基于两种柔性同分异构羧酸配体的钴(Ⅱ)配合物的合成、结构及磁性研究

马志峰 章应辉 胡同亮* 卜显和
(南开大学化学系,金属与分子基材料化学天津市重点实验室,天津 300071)

摘要: 分别以 *E*-3-[4-(羧甲氧基)-苯基]丙烯酸(H_2L^1)和 *E*-3-[3-(羧甲氧基)-苯基]丙烯酸(H_2L^2)为主配体,合成了 3 种钴(Ⅱ)配位聚合物:$[Co(L^1)(bpp)]_n$(**1**),$\{[Co(\mu_3\text{-}OH)_2(L^2)_4(bpy)_2(H_2O)_4]\cdot 12H_2O\}_n$(**2**)和$[Co(L^2)(bpy)]_n$(**3**)(bpp: 1, 3-二吡啶基丙烷, bpy: 4,4-联吡啶)。通过元素分析、红外光谱、X 射线粉末和单晶衍射对其进行了结构表征。结果表明钴(Ⅱ)离子在这 3 种配合物中具有不同的配位环境,导致 3 种配合物具有不同的晶体结构和磁性特征。

关键词: 钴(Ⅱ)配合物; 柔性配体; 晶体结构; 磁性
中图分类号: O614.81+2 **文献标识码**: A **文章编号**: 1001-4861(2014)01-0204-09
DOI:10.11862/CJIC.2014.078

Three Cobalt(Ⅱ) Complexes Based on Isomeric Carboxylate-Based Flexible Ligands: Syntheses, Structures and Magnetism

MA Zhi-Feng ZHANG Ying-Hui HU Tong-Liang* BU Xian-He
(*Department of Chemistry, and Tianjin Key Laboratory of Metal & Molecule-based Material Chemistry, Nankai University, Tianjin* 300071, *china*)

Abstract: Three Co(Ⅱ) complexes based on *E*-3-[3-(carboxymethoxy)-phenyl]acrylic acid (H_2L^1) or *E*-3-[3-(carboxymethoxy)-phenyl]acrylic acid (H_2L^2), namely $[Co(L^1)(bpp)]_n$(**1**), $\{[Co(\mu_3\text{-}OH)_2(L^2)_4(bpy)_2(H_2O)_4]\cdot 12H_2O\}_n$ (**2**), and $[Co(L^2)(bpy)]_n$(**3**) (bpp: 1,3-bi(pyridin-4-yl)propane, bpy: 4,4-bipyridine), were synthesized and characterized by elemental analysis, IR, XRPD and X-ray single-crystal structure analysis. Different coordination environment for Co(Ⅱ) ions and thereby different crystal structures and magnetism were observed for these three complexes. The magnetic properties of complexes **1** and **2** were discussed in detail. CCDC: 964873, **1**; 964875, **2**; 964876, **3**.

Key words: cobalt(Ⅱ) complexes; flexible ligands; crystal structure; magnetic property

0 Introduction

In the past two decades, diversified coordination polymers with special structures and properties have been designed and synthesized [1-5], owing to their potential application in many fields, such as gas adsorption and separation, catalysis, electronic and magnetic devices, and molecular recognition [6-11]. Though great advances have been made, synthesizing target compound with designed structure and properties still remains as a fascinating challenge in this field. To achieve this goal, choosing carefully

收稿日期:2013-11-18。收修改稿日期:2013-11-30。
国家自然科学基金(No.21031002)和天津市自然科学基金(No.11JCYBJC041000)资助项目。
*通讯联系人。E-mail:022-23502458;E-mail: tlhu@nankai.edu.cn;会员登记号:S06N9133M1005。

suitable metal ions and organic ligands is necessary[12-15]. The most popular ligands used in constructing predesigned coordination polymers are those with rigid backbone, which commonly facilitates the directed assembling of metal ion and ligands into designed structure, especially in the construction of porous coordination polymers[16-18]. Whereas, those ligands with flexible geometry, being apt to promote the occurrence of interpenetration that reduces the porosity, attracted relatively little attention. However, flexible ligands, producing polymers of intriguing geometry and novel properties in some cases [19-20], are of benefit to the structural diversity of coordination polymers and therefore gaining increasing interest.

Carboxylate group is one of the most used coordination group in constructing coordination complexes, owing to its abundant coordination modes such as monodentate, bidentate and chelate [21-23]. Most recently, many carboxylate-based flexible ligands have been designed and synthesized in this field. Among these ligands *E*-3-[3-(carboxymethoxy)-phenyl]acrylic acid (H_2L^2) used in constructing some two-dimensional (2D) Zn (Ⅱ) and Mn (Ⅱ) complexes [24-26], attracts our attention by its variable coordination modes of two different carboxylate acid group. In this paper, we design an isomeric ligand of H_2L^2, *E*-3-[4-(carboxymethoxy)-phenyl]acrylic acid (H_2L^1) (Chart 1). By varying reaction condition, three new Co (Ⅱ) coordination polymers, $[Co(L^1)(bpp)]_n$ (**1**), $\{[Co(\mu_3\text{-}OH)_2(L^2)_4(bpy)_2(H_2O)_4]\cdot 12H_2O\}_n$ (**2**), and $[Co(L^2)(bpy)]_n$ (**3**) (bpp: 1,3-bi(pyridin-4-yl)propane, bpy: 4,4-bipyridine), were obtained with different coordination environment for Co (Ⅱ). Meanwhile, the magnetic properties of complexes **1** and **2** were discussed in detail.

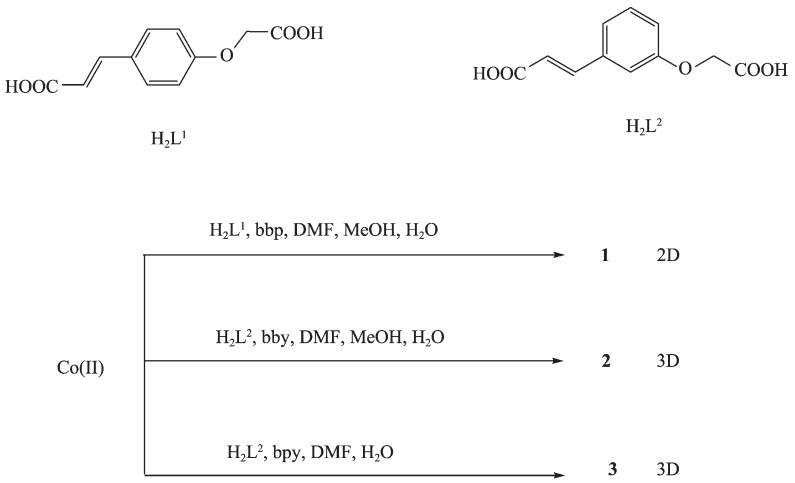

Chart 1　Structures of H_2L^1 and H_2L^2 and the syntheticconditions of complexes **1~3**

1　Experimental

1.1　Materials and general methods

All reagents and solvents for synthesis were used as received or purified by standard methods prior to use. Elemental analyses (C, H and N) were performed on a Perkin-Elemer 240 Canalyzer. The IR spectra were measured on a Tensor 27 OPUS (Bruker) FTIR spectrometer with KBr pellets. The measurement of magnetism was carried out by MPMS-XL-7 magnetometer. The X-ray powder diffraction (XRPD) were recorded on a Rigaku D/Max-2500 diffractometer operated at 40 kV and 100 mA, using a Cu-target tube and a graphite monochromator. The intensity data were collected by continuous scan in a $2\theta/\theta$ mode from 5° to 35°, with a step size of 0.02° and a scan speed of $8°\cdot min^{-1}$.

1.2　Synthesis

1.2.1　Synthesis of ligands $H_2L^1$and H_2L^2

The synthesis of H_2L^2 was carried out according to literature [24]. H_2L^1 was synthesized in a similar method except replacing 3-(3-hydroxyphenyl)-2-

propenoic acid by 3-(4-hydroxyphenyl)-2-propenoic acid with a yield of 80%. IR (KBr pellet, cm^{-1}): H_2L^1: 3 126(b), 2 360(m), 1 653(w), 1 559(w), 1 497(w), 1 398 (vs), 810(m), 750(m); H_2L^2: 3 357(b), 2 354(m), 1 653 (w), 1 591(w), 1 559(w), 1 497(w), 1 454(w), 1 398(vs), 796(m), 643(m).

1.2.2 Synthesis of $[Co(L^1)(bpp)]_n$ (**1**)

H_2L^1 (22 mg, 0.1 mmol), bpp (19.6 mg, 0.1 mmol), and $Co(NO_3)_2\cdot 6H_2O$ (29 mg, 0.1 mmol) were added in a mixing solution of DMF, water and methanol (1∶1∶1, *V*/*V*, 6 mL). The vial was sealed and heated at 100 ℃ for two days. After being cooled to room temperature, dark purple crystals were obtained in 40% yields. Anal. Calcd for $C_{24}H_{20}CoN_2O_5$ (%): C, 46.93; H, 3.94; Found (%): C, 46.36; H, 3.58. FTIR (KBr pellet, cm^{-1}): 3 458(b), 2 369(s), 1 613(s), 1 427 (vs), 1 215(w), 984(w), 815(w), 612(m), 505(m).

1.2.3 Synthesis of $\{[Co(\mu_3\text{-}OH)_2(L^2)_4(bpy)_2(H_2O)_4]\cdot 12H_2O\}_n$ (**2**)

The synthesis of complex 2 was carried out in the similar procedure to that of complex **1**, except replacing ligand H_2L^1 and bpp with H_2L^2 and bpy in same molar quantities. After reaction, dark red crystals were obtained in 35% yield. Anal. Calcd. for $C_{64}H_{70}Co_5N_4O_{38}$ (%): C, 42.75; H, 3.92; N, 3.11; Found (%): C, 41.36; H, 3.68; N, 3.24. FTIR (KBr pellet, cm^{-1}): 3 453(b), 2 355(s), 1 658(s), 1 476(vs), 1 384 (w), 975(w), 672(m).

1.2.3 Synthesis of $[Co(L^2)(bpy)]_n$ (**3**)

H_2L^2 (22 mg, 0.1 mmol), 4,4-bpy (15.6 mg, 0.1 mmol), and $Co(NO_3)_2\cdot 6H_2O$ (29 mg, 0.1 mmol) were added in a mixing solution of DMF and H_2O (1∶1, *V*/*V*, 6 mL). The vial was sealed and heated in oven at 100 ℃ for four days. After being cooled to room temperature, dark red crystals were obtained in 70% yield. Anal. Calcd. for $C_{21}H_{16}CoN_2O_5$ (%): C, 57.94; H, 3.70; N, 6.44; Found (%): 57.32; H, 3.57; N, 6.18 %. FTIR (KBr pellet, cm^{-1}): 3 388(b), 2 350(s), 1 613(s), 1 447(vs), 1 136(w), 815(w), 620(m).

1.3 Crystal structure determination

Single-crystal X-ray diffraction measurements were carried out on a Rigaku SCX-mini diffractometer. The diffraction data were collected with Mo *Kα* radiation (*λ* =0.071 073 nm). Empirical absorption corrections were carried out by using the SADABS program.[27] The unit cell dimensions were determined by direct methods using the SHELXS program of the SHELXTL package and refined with SHELXL[28]. All non-hydrogen atoms were refined anisotropically. The hydrogen atoms were added theoretically, riding on the concerned atoms and refined with fixed thermal factors. Crystallographic data and experimental details for structural analyses are summarized in Table 1. Some selected structural parameters are collected in Table 2.

CCDC: 964873, **1**; 964875, **2**; 964876, **3**.

Table 1 Crystal parameters of coordination complexes 1~3

Complex	**1**	**2**	**3**
Formula	$C_{24}H_{20}CoN_2O_5$	$C_{64}H_{70}Co_5N_4O_{38}$	$C_{21}H_{16}CoN_2O_5$
Molecular weight	475.35	1 797.91	435.29
Crystal system	Monoclinic	Monoclinic	Monoclinic
Space group	$P2_1/n$	$P2_1/c$	$C2/c$
a / nm	1.151 8(2)	1.184 2(2)	2.081 2(4)
b / nm	1.058 5(2)	1.175 9(2)	0.920 7(18)
c / nm	1.804 1(4)	2.743 2(8)	2.217 8(4)
α / (°)	90	90	90
β / (°)	90.54(3)	102.48	104.60(3)
γ / (°)	90	90	90
V / nm^3	2.199 4(7)	3.729 6	4.112 5
Z	4	2	8
D_c / ($g\cdot cm^{-3}$)	1.436	1.513	0.862

Continued Table 1

Absorption coefficient / mm^{-1}	0.818	1.183	1.743
T / K	293(2)	293(2)	293(2)
F(000)	980.0	1 674	1 640
Reflections collected	18 075	30 282	21 045
Independent inflections	3 847	6 552	4 707
Parameters	289	502	262
R_{int}	0.094 2	0.053 9	0.068 0
Final R indices ($I>2\sigma(I)$)	0.069 0	0.047 4	0.077 6
wR (all data)	0.193 9	0.117 4	0.235 5
GOF on F^2	1.101	1.081	1.090

Table 2　Selected bond distances (nm) and bond angle (°) for complexes 1~3

			1		
Co(1)-O(4)	0.209 5(4)	Co(1)-O(3)	0.210 4(4)	Co(1)-O(1)	0.214 5(5)
Co(1)-O(2)	0.222 0(5)	Co(1)-N(2)	0.216 1(6)	Co(1)-N(1)	0.216 1(6)
O(1)-Co(1)-O(2)	60.50(18)	O(3)-Co(1)-O(2)	90.76(18)	O(4)-Co(1)-O(2)	91.80(18)
O(1)-Co(1)-N(1)	109.5(2)	O(3)-Co(1)-N(1)	86.02(19)	O(4)-Co(1)-N(1)	91.85(19)
O(1)-Co(1)-N(2)	157.0(2)	O(3)-Co(1)-N(2)	88.09(19)	O(4)-Co(1)-N(2)	89.42(19)
N(1)-Co(1)-O(2)	169.4(2)	N(2)-Co(1)-O(2)	96.5(2)		
			2		
Co(3)-O(5)^{i}	0.209 1(3)	Co(3)-O(1)	0.209 3(2)	Co(3)-O(10)	0.211 9(3)
Co(3)-O(2)	0.212 9(2)	Co(3)-N(2)^{ii}	0.214 4(3)	Co(3)-O(11)	0.215 6(3)
Co(2)-O(4)^{i}	0.209 6(3)	Co(2)-O(9)^{iii}	0.209 8(3)	Co(1)-O(1)^{iv}	0.210 0(2)
Co(1)-O(7)^{iv}	0.215 5(3)	Co(1)-O(8)^{iii}	0.216 2(2)		
O(5)^{i}-Co(3)-O(1)	89.41(10)	O(5)^{i}-Co(3)-O(10)	178.67(11)	O(1)-Co(3)-O(10)	91.35(10)
O(5)^{i}-Co(3)-O(2)	91.38(10)	O(1)-Co(3)-O(2)	83.45(10)	O(10)-Co(3)-N(2)^{ii}	94.00(12)
O(2)-Co(3)-N(2)^{ii}	176.28(12)	O(10)-Co(3)-O(2)	106.06(18)	O(5)^{i}-Co(3)-N(2)^{ii}	86.94(12)
O(1)-Co(3)-N(2)^{ii}	99.84(11)	O(5)^{i}-Co(3)-O(11)	89.44(11)		
			3		
Co(1)-O(6)^{i}	0.200 9(4)	Co(1)-O(5)^{ii}	0.202 3(4)	Co(1)-N(2)^{iii}	0.214 6(4)
Co(1)-N(1)	0.214 8(4)	Co(1)-O(3)	0.215 1(4)	Co(1)-O(4)	0.251 9(6)
O(6)^{i}Co(1)-O(5)^{ii}	115.90(17)	O(6)^{i}-Co(1)-N(2)^{iii}	87.13(15)	O(5)^{ii}-Co(1)-N(2)^{iii}	89.28(16)
O(6)^{i}-Co(1)-N(1)	92.65(16)	O(5)^{ii}-Co(1)-N(1)	93.17(16)	N(2)^{iii}-Co(1)-N(1)	177.37(17)
N(2)^{iii}-Co(1)-O(3)	90.99(17)	O(5)^{ii}-Co(1)-O(3)	90.87(17)	O(6)^{i}-Co(1)-O(3)	153.12(17)
N(2)^{iii}-Co(1)-O(4)	85.20(16)	N(1)-Co(1)-O(4)	92.20(17)	O(3)-Co(1)-O(4)	59.52(16)

symmetry transformations used to generate equivalent atoms: for **2**: ^{i} 1−x, −0.5+y, 1.5−z; ^{ii} −x, 0.5−y, 0.5+z; ^{iii} x, 1.5−y, 0.5+z; ^{iv} 2−x, 1−y, 2−z. **3**: ^{i} x, 1−y, 0.5+z; ^{ii} 2−x, −1+y, 0.5−z; ^{iii} 0.5+x, −0.5−y, z

2　Results and discussion

2.1　Description of crystal structure

2.1.1　Crystal structure of complex **1**

Single-crystal X-ray diffraction measurements indicated that complex **1** crystallizes in $P2_1/n$ space group, and the asymmetric unit of **1** composes a Co(Ⅱ) ion, an L^1 ligand, and a bpp ligand. The Co(Ⅱ) is

coordinated by two N atoms from two bpp ligands, two monodentate O atoms from two phenoxyacetate groups and chelated by an anacrylate group, to form a distorted octahedron (Fig.1a). The Co-O/N bond distances (0.209 5~0.222 0 nm) are within the normal range. Its worth noticing that two different coordination modes were observed for carboxylate groups in this complex. One is bridging two adjacent metal ions by the phenoxyacetate group to form a 1D chain, while the other is chelating one metal ion by the acrylate group. The latter chelating mode, together with the coordination effect of bpp, extends the 1D Co(Ⅱ) chain into a 2D network (Fig.1c). Interestingly, the Co(Ⅱ) chain, linked by bpp or L^1 ligand, exhibits a helical structure (Fig.1b). The chirality of the helical chains is homogeneous in the same 2D net plane, but is opposite to that of the adjacent plane (Fig.1c), which generates the final mesomeric complex **1**.

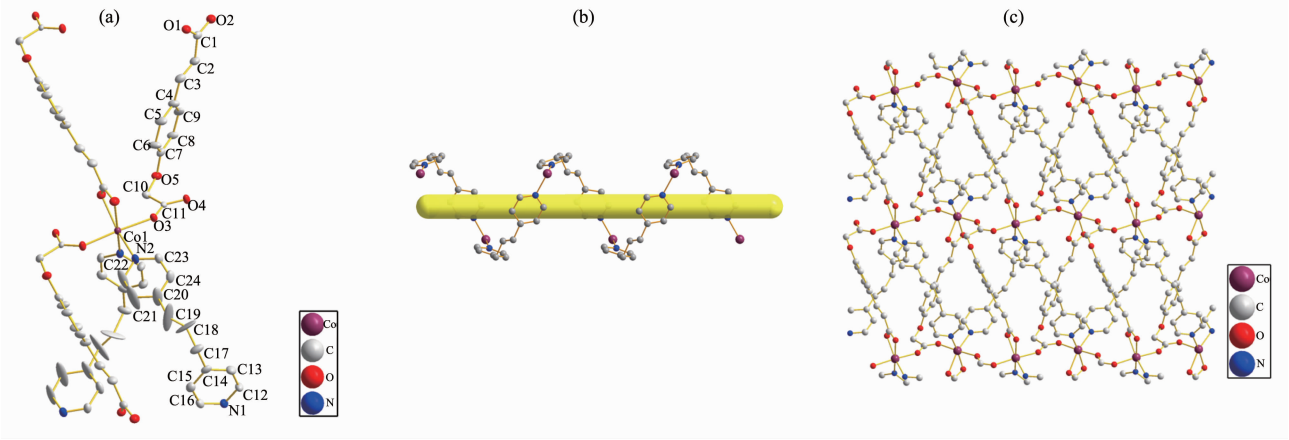

Displacement ellipsoids are drawn at the 30% probability level in (a)

Fig.1 (a) coordination environment of Co(Ⅱ) ion in **1**; (b) the 1D helical chain formed between Co(Ⅱ) ions and bpp ligands; (c) the 2D network of **1**

2.1.2 Crystal structure of complex **2**

Complex **2** crystallizes in $P2_1/c$ space group. The asymmetric unit composes a penta-nuclear Co (Ⅱ) cluster, four L^2 anions, two bpy molecules, two μ_3-OH ions, four coordinating water molecules and twelve lattice water molecules, as shown in Fig.2a. The penta-nuclear Co (Ⅱ) cluster comprises three kinds of crystallographic independent Co(Ⅱ) ions. All five Co(Ⅱ) ions are coplanar and were hexa-coordinated with six carboxylate groups, two μ_3-OH groups and four half bpy molecules. The Co1 locates in the center of the cluster and is surrounded by other four Co atoms, namely Co2, Co3, Co2′, Co3′ (Co1⋯Co2 0.387 8 nm, Co1⋯Co3 0.3550 nm, Co2 ⋯ Co3 0.3107 nm, Co2-Co1-Co3 114.34°, Co2-Co1-Co3′ 130.84°, Co3-Co1-Co2′ 130.84°). Co1 is linked with Co3 (Co3′) by a μ_3-OH group, and with Co2 (Co2′) by a couple of OCO groups together with a μ_3-OH group, while Co2 (Co2′) is linked with Co3(Co3′) by a μ_2-$O_{carboxyl}$ group and an OCO group. Meanwhile, Co3(Co3′) is coordinated with two terminal H_2O molecules. Furthermore, one penta-nuclear cluster was linked with neighboring four ones by either an L^2 and four bpys, to form a 3D network that can be simplified as a $4^{24}\cdot6^4$ topographic structure by simplifying the penta-nuclear cluster as one node, as indicated in Fig.2c. In complex **2**, only bridging coordination mode was found for carboxylic group.

2.1.3 Crystal structure of complex **3**

Similar reaction to the synthesis of complex **2**, except the addition of methanol, produces complex **3** that crystallizes in $C2/c$ space group based on bi-nuclear Co unit. This testifies the key influence of the solvent to production. The asymmetric unit of complex **3** composes one Co(Ⅱ) ion, one L^2 ligand and one bpy ligand. The Co(Ⅱ) ion is hexa-coordinated by two N atoms from two bpy ligands, two monodentate O atoms

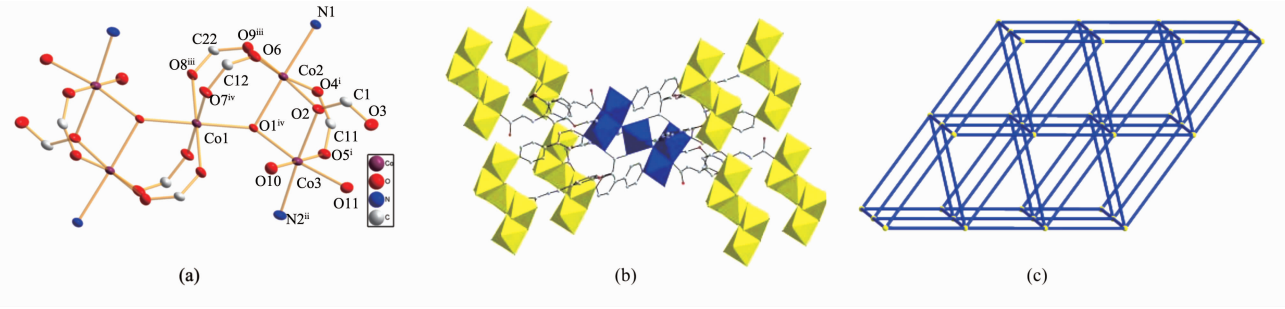

Displacement ellipsoids are drawn at the 30% probability level in (a); Symmetry code: [i] 1–*x*, –0.5+*y*, 1.5–*z*; [ii] –*x*, 0.5–*y*, 0.5+*z*; [iii] *x*, 1.5–*y*, 0.5+*z*; [iv] 2–*x*, 1–*y*, 2–*z*

Fig.2　(a) coordination environment of penta-nuclear Co(Ⅱ) cluster in **2**; (b) the 3D network based on penta-nuclear clusters; (c)the topographic structure of **2**

from two L^2 ligands, and two chelating O atoms from one L^2 ligand, to form an octahedron coordination configuration (see Fig.3a, b). Similar to the performance of L^1 in complex **1**, two kinds of coordination modes were observed for the carboxylic group of L^2 in **4**. One is the bridging linking of two adjacent Co(Ⅱ) ions with a couple of acrylate groups to produce a cyclic bi-nuclear Co(Ⅱ) unit; the other is the chelating of one Co(Ⅱ) ion by a phenoxyacetate group. These coordination modes produce a 2D layer (see Fig.3c) that was further extended to 3D network (see Fig.4d) by the coordination of auxiliary bpy ligands.

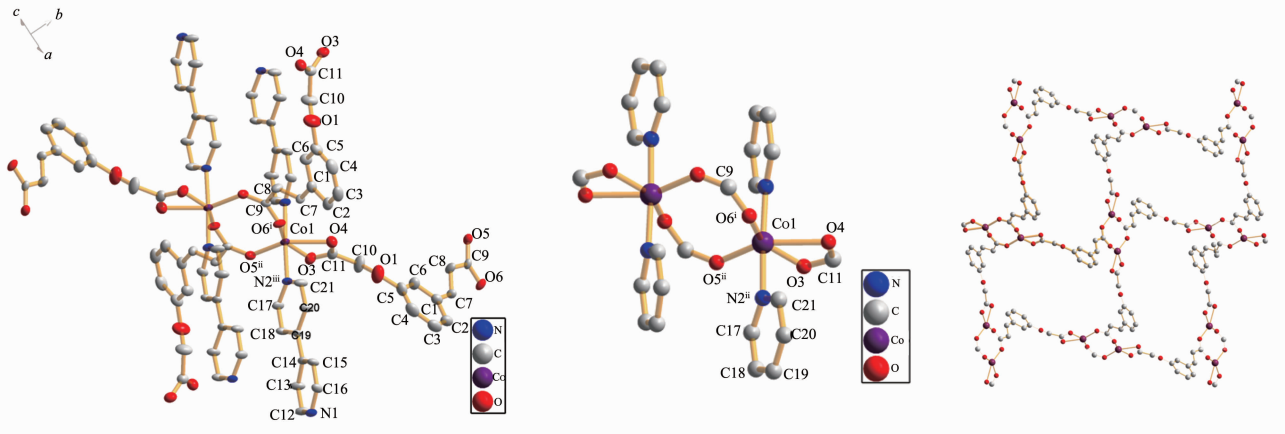

Displacement ellipsoids are drawn at the 30% probability level in (a); Symmetry code: [i] *x*, 1–*y*, 0.5+*z*; [ii] 2–*x*, –1+*y*, 0.5–*z*; [iii] 0.5+*x*, –0.5–*y*, *z*

Fig.3　(a) coordination structure of Co(Ⅱ) in asymmetric unit of **3**; (b) the bi-nuclear Co(Ⅱ) structure; (c) the 2D network formed by the coordination of Co(Ⅱ) with carboxylate group

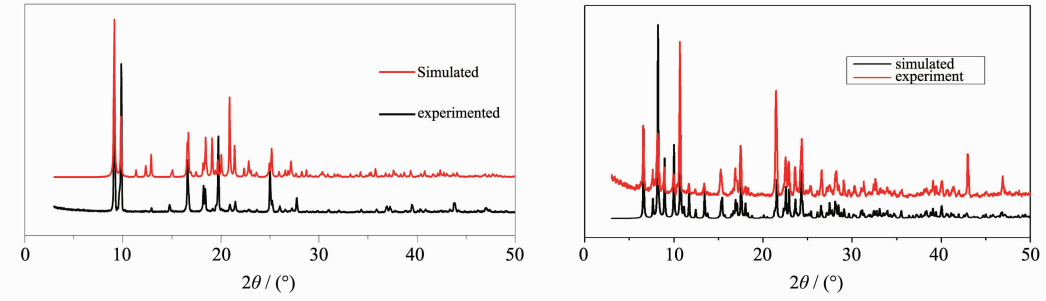

Fig.4　XRPD patterns of complexes (a) **1** and (b) **2**

2.2 XRPD of coordination complexes

In order to make sure the crystal structure is truly representative of the bulk materials used in the following luminescence and magnetic measurement, the XRPD was measured for complexes **1** and **2** (see Fig.4). Inspection of Fig.4 indicates that the experimental diffraction pattern is in well consistent with the simulated pattern from single crystal data, which manifests the bulky solid sample used for properties measurement is homogeneous.

2.3 Magnetic properties of complexes **1** and **2**

The molar magnetic susceptibilities of **1** and **2** were measured at an applied magnetic field of 2 kOe in the temperature range of 2~300 K (see Figures 5a and 6a). Inspecting Fig.6a and 7a shows the $\chi_M T$ value of 3.53 emu·K·mol^{-1} and 2.93 emu·K·mol^{-1} for complexes **1** and **2** at 300 K, which are much larger than the expected spin-only value (1.875 emu·K·mol^{-1}) for a single Co(Ⅱ) ion at g=2.0, indicating strong spin-orbits coupling among Co(Ⅱ) ions in complexes **1** and **2**.

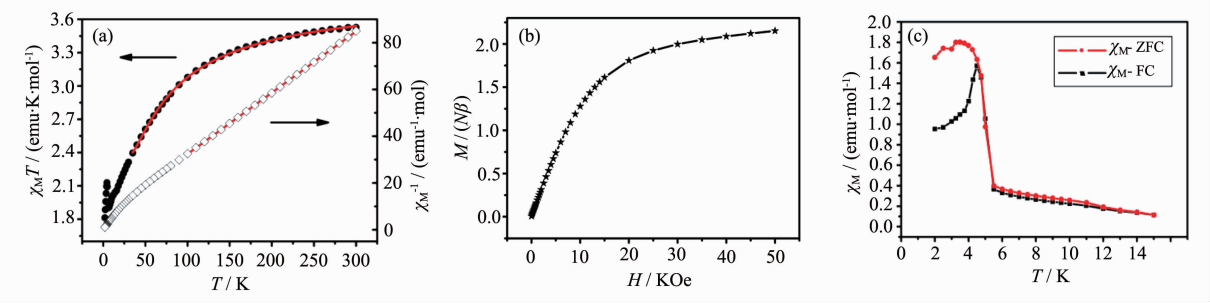

Fig.5 (a) $\chi_M T$ vs T and χ_M^{-1} vs T plot of **1** at 0.1T (the red profile is the Currier-Weiss fitting profile); (b) the M vs H plot of **1** at 2 K; (c) the temperature dependence of the field cooled (FC) and zero-field-cooled (ZFC) magnetization of **1** under a field of 50 Oe

Best Curie-Weiss fitting (χ_M=C/(T−θ)) for the data in the range of 100~300 K results in C=3.81 emu·K·mol^{-1} and θ=−23.43 K for **1** and C=16.77 emu·K·mol^{-1} and θ=−41.83 K for **2**. The negative value of Weiss constant θ should be attributed to the strong spin-orbit coupling other than antiferromagnetic interaction.[29] Its general known that spin-orbit coupling could bring about antiferromagnetic interaction of Co(Ⅱ) ions at high temperature region (35 ~300 K), which can be estimated by following equation[29].

$$\chi_M T = A\exp(-E_1/(kT))+B\exp(-E_2/(kT))$$

Where, A +B equals to Curie-Weiss constant, E_1 and E_2 represent the active energy for the spin-orbit coupling and antiferromagnetic super exchange interaction, respectively. The best fitting to the experimental data gives A +B=3.81 emu·K·mol^{-1}, E_1/k =−26.76 K, E_2/k =45.98 K for **1**, and A +B =16.81 emu·K·mol^{-1}, E_1/k =−59.74 K, E_2/k =19.34 K for **2**, respectively. The positive value of E_2 clarifies the ferromagnetic interaction among adjacent Co(Ⅱ) ions for complexes **1** and **2**.

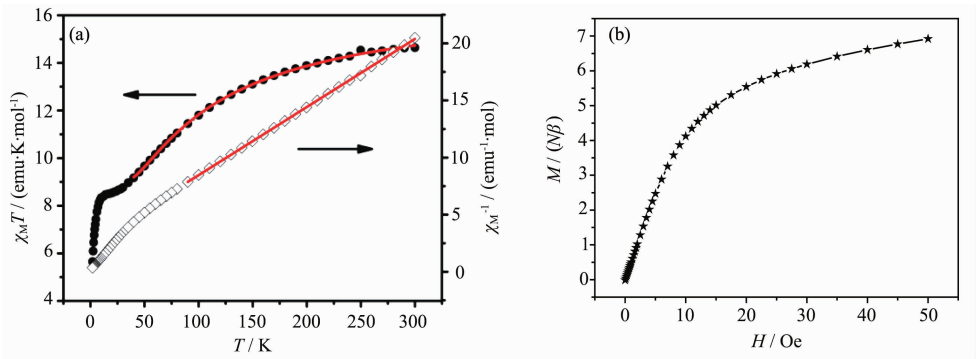

Fig.6 (a) $\chi_M T$ vs T and χ_M^{-1} vs T plot of **2** at 0.1T (the red profile is the best Currier-Weiss fitting profile); (b) the M vs H plot of **2** at 2 K

For complex **1**, with the decreasing of temperature, $\chi_M T$ value decreases slowly down to a minimum of 1.90 emu·K·mol^{-1} at about 6 K (see Fig. 5a), due to strong spin-orbit coupling. Below 6 K, the $\chi_M T$ value increases quickly to a maximum of 2.13 emu·K·mol^{-1} at about 4.5 K, which may be attributed to the ferromagnetic interaction among Co(Ⅱ) ions under this condition. The finally quick decrease of the $\chi_M T$ value to 1.8 emu·K·mol^{-1} at 2 K may be ascribed to the combined effect of magnetic saturation and (or) antiferromagnetic interaction. For complex **2**, with the decreasing of temperature, the $\chi_M T$ value decreases slowly down to a minimum of 5.65 emu·K·mol^{-1} at about 2 K (see Fig.6a), owing to antiferromagnetic interaction.

Complex **1** is a 2D coordination polymer based on 1D Co(Ⅱ) chains. The overall ferromagnetic property of **1** composes the ferromagnetic interaction among the Co(Ⅱ) ions within the same 1D Co chain and the antiferromagnetic interaction between 1D Co chains. The plot of M vs. H (Fig.5b) shows an increasing of M value with the increasing magnetic fields at 2 K. The 2.13$N\beta$ of M at 5 T close to the saturate value ($2N\beta$) of a octahedron Co(Ⅱ), which further testifies the ferromagnetic interaction among the Co(Ⅱ) ions in a Co(Ⅱ) chain. Similar increase of M was also observed for complex **2** but with a smaller value of M at 5 T (only 6.92$N\beta$ for the penta-nuclear cluster), indicating the sub-ferromagnetism of **2** (see Fig.6b).

In order to further clarify the magnetic properties of **1**, the ZFC and FC profiles were measured under a field of 50 Oe (see Fig.5c). The derivation of ZFC profile from FC profile at about 4.5 K manifests the existence of magnetic phase-transformation[30], revealing the long distance ordering ferromagnetism for **1**[31].

3 Conclusion

In summary, three Co(Ⅱ) coordination polymers based on a pair of isomeric (carboxymethoxy)-phenylacrylic acid ligands (H_2L^1 and H_2L^2) were synthesized and characterized, with different coordination environment for Co(Ⅱ) ions and crystal structure. This highlights the vital influence of reaction condition to the coordination polymers. The ferromagnetism and sub-ferromagnetism were found for complexes **1** and **2**, respectively.

Acknowledgements: This work was financially supported by NSFC (21031002) and the NSF of Tianjin, China (11JCYBJC04100).

References:

[1] Karmakar T K, Ghosh B K, Usman A, et al. *Inorg. Chem.*, **2005**,**44**:2391-2393

[2] Das A, Rosair G M, Fallah M S E, et al. *Inorg. Chem.*, **2006**,**45**:3301-3306

[3] Chen Q, Chang Z, Bu X H, et al. *Angew. Chem. Int. Ed.*, **2013**,**52**,11550-11553

[4] Hagen K S, Naik S G, Huynh B H, et al. *J. Am. Chem. Soc.*, **2009**,**131**:7516-7517

[5] Zeng Y F, Hu X, Bu X H, et al. *Chem. Soc. Rev.*, **2009**,**38**:469-480

[6] Banerjee R, Phan A, Wang B, et al. *Science*, **2008**,**319**:939-943

[7] Férey G, Mellot-Draznieks C, Serre C, et al. *Acc. Chem. Res.*, **2005**,**38**:217-225

[8] Wu C, Hu A, Lin W. *J. Am. Chem. Soc.*, **2005**,**127**:8940-8941

[9] Wu C, Lin W. *Angew. Chem. Int. Ed.*, **2007**,**46**:1075-1078

[10]Ma L, Mihalcik D J, Lin W. *J. Am. Chem. Soc.*, **2009**,**131**:4610-4612

[11]Chen Y Q, Li G R, Bu X H, et al. *Chem. Sci.*, **2013**,**4**:3678-368

[12]Zhang P, Zhang L, Lin S Y, et al. *Inorg. Chem.*, **2013**,**52**:4587-4592

[13]Kaminker R, Motiei L, Gulino A, et al. *J. Am. Chem. Soc.*, **2010**,**132**:14554-14561

[14]Li J R, Tao Y, Bu X H, et al. *Chem. Commun.*, **2007**:1527-1529

[15]Tian D, Chen Q, Bu X H, et al. *Angew. Chem. Int. Edit.*, **2013**,DOI: 10.1002/anie.201307681

[16]Baur W H. *Nat. Mater.*, **2003**,**2**:17-18

[17]Yao X Q, Cao D P, Hu J S, et al. *Cryst. Growth Des.*, **2011**,**11**:231-239

[18]Thomas D, Serre C, Audebrand N, et al. *J. Am. Chem. Soc.*, **2005**,**127**:1278812789

[19]Seo J S, Whang D, Lee H, et al. *Nature*, **2000**,**404**:982-986

[20]Ghosh S K, Zhang J P, Kitagawa S. *Angew. Chem. Int. Ed.*, **2008**,**47**:3403-3406

[21]Fang S M, Zhang Q, Hu M, et al. *Inorg. Chem.*, **2010**,**49**:

9617-9626

[22]Eliseeva S V, Pleshkov D N, Lyssenko K A, et al. *Inorg. Chem.*, **2010**,**49**:9300-9311

[23]Blight B A, Stewart A F, Wang N, et al. *Inorg. Chem.*, **2012**,**51**:778-780

[24]Zheng X Y, Ye L Q, Wen Y H. *J. Mol. Struct.*, **2011**,**987**:132-137

[25]Chen L. *Acta Cryst. E*, **2012**,**68**:m882

[26]Ji J, Yang Y F, Wen Y H. *Acta Cryst. E*, **2012**,**68**:m912-913

[27]Sheldrick G M. *SADABS, Siemens Area Detector Absorption Corrected Software*, University of Gttingen, Germany, **1996**.

[28]Sheldrick G M. *SHELXTL NT Version* 5.1. *Program for Solution and Refinement of Crystal Structures*, University of Gttingen, Germany, **1997**.

[29]Liu S J, Xue L, Hu T L, et al. *Dalton Trans.*, **2012**,**41**:6813-6819

[30]Wang X Y, Wang Z M, Gao S. *Inorg. Chem.*, **2008**,**47**:5720-5726

[31]Cheng X H, Xue W, Zhang W X, et al. *Chem. Mater.*, **2008**,**20**:5345-5350